

1 Summary

- Accurately predicting ground motions for future large earthquakes is crucial for seismic hazard analysis and limited data necessitates ground motion simulations.
- **Dynamic simulations** – Physically accurate but computationally demanding
- **Kinematic simulations** - Efficient yet rely on predefined slip evolution.
- **Pseudo-Dynamic simulations (PD)** - Integrating physics-compatible source within a kinematic approach (Guatteri et al., 2004; Graves and Pitarka 2010; 2016; Song et al., 2013).
- We present a machine learning (ML) based PD rupture generator framework to analyze the following earthquake source parameters:
 - Rupture velocity
 - Peak slip velocity
 - Modifications to source time function (STF)
- Validation for M_w 6.5 strike-slip scenario using NGA West 2 Ground motion models (GMMs).

2 Dataset description

- We use dynamic rupture simulations on vertical rough strike-slip fault from Mai et al., (2018) with 21 source models across 3 roughness realizations and 3 hypocentre locations.
- For our study, we use 15 source models for training and 6 for validation.
- Figure 1 show rupture parameters - Slip, Rupture speed (V_r), Peak slip velocity (PSV) and Rise time (Tr) extracted from the dynamic rupture simulation (Mai et al., 2018).

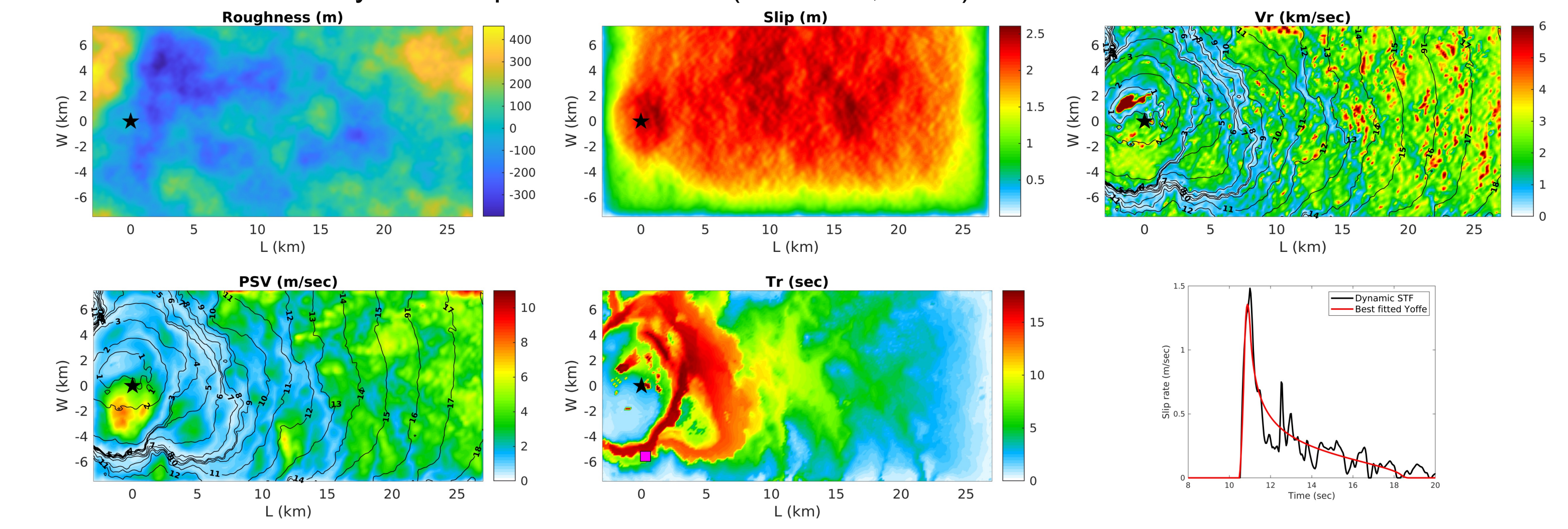


Figure 1. Roughness and rupture parameters (Slip, V_r , PSV and Tr) extracted from dynamic rupture simulation (Mai et al., 2018). Rise time is computed from a best fitting Yoffe to dynamic STF (bottom right).

3 Earthquake source parameters

A. Rupture Velocity

- Dynamic rupture simulations show rupture deceleration (acceleration) in regions of variable roughness gradient, coinciding with fault areas of increased (decreased) on-fault shear stresses.
- We train a ML framework involving Fourier Neural Operators (FNO) (Li et al., 2020), establishing relations between, static stress drop, hypocentre distance and V_r (Figure 2).
- Figure 3 shows the Machine Learning estimations for two test cases.

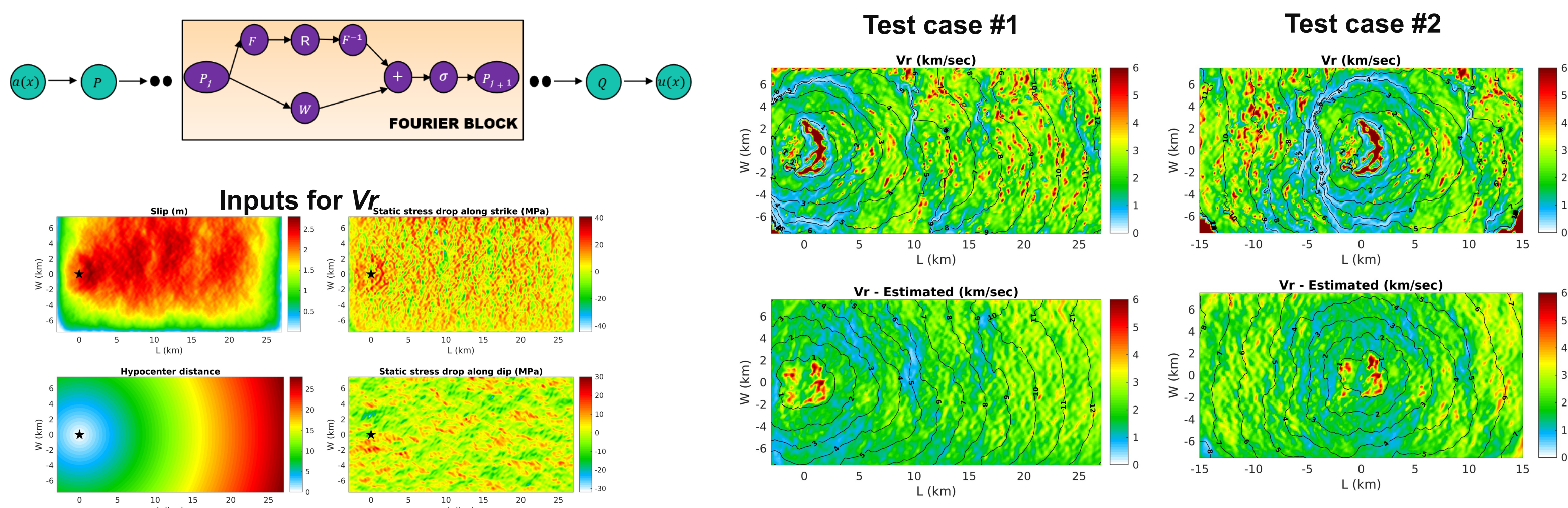


Figure 2. Fourier Neural Operator (FNO) architecture used in this study (Top). Inputs to the V_r model are static stress drop along strike and dip directions and hypocenter distance.

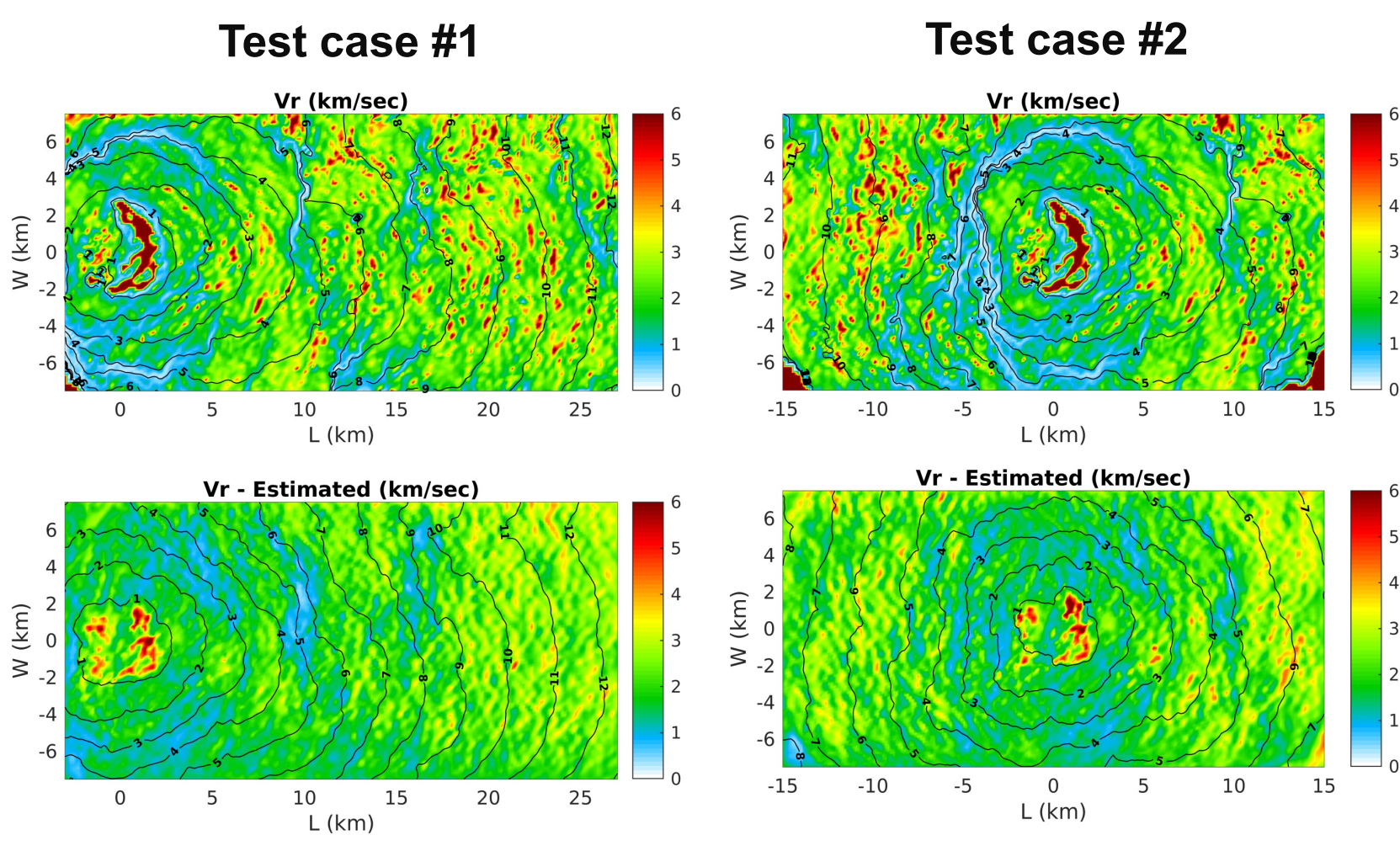


Figure 3. Machine learning estimations for V_r for two test cases. The top row represents original rupture speed whereas bottom row are the estimates. Onset times are obtained using a fast-marching algorithm.

B. Peak slip velocity and Rise Time

- PSV is closely correlated with V_r (Figure 1) and hence, we train a FNO model (Figure 2) relating V_r with PSV .
- We limit the $max(PSV)$ to be 5 m/s following Andrews et al., (2005).
- Assuming a Yoffe STF, we calculate Tr empirically from Tinti et al., (2005) using
- Figure 4 show ML estimated PSV and Tr for two test cases.

$$Tr = \sqrt[0.47]{\frac{1.04 (slip)}{(PSV) (Tacc)^{0.54}}}$$

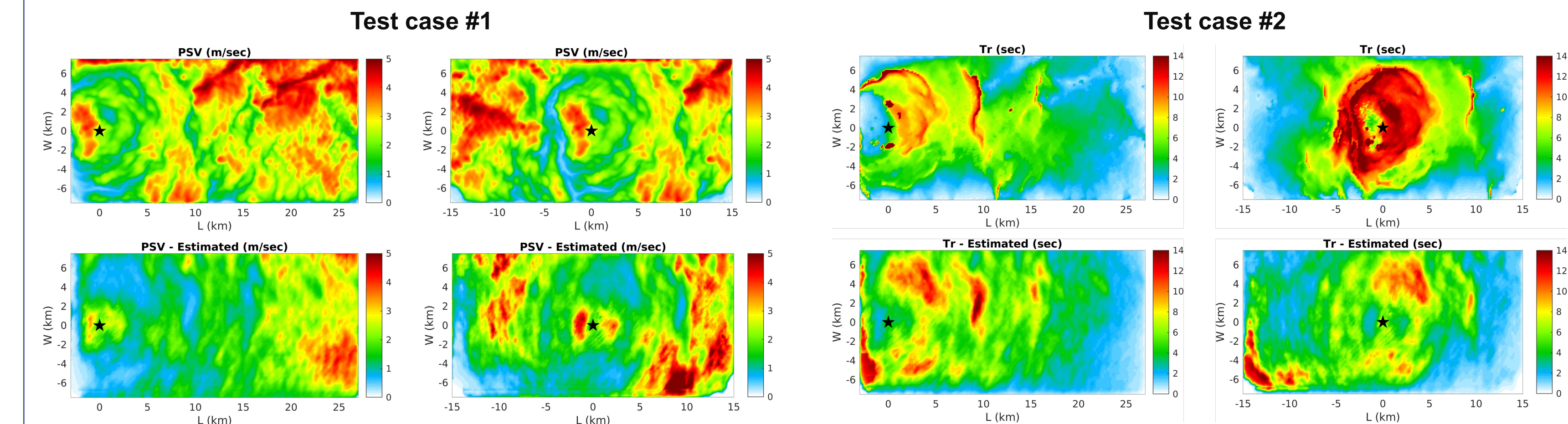


Figure 4. Machine learning estimates for PSV (Left group) and Tr (Right group). Top row and bottom row represents original and estimated parameters.

C. Modifications to STF

- Large and small scale variations in the STF affect wavefield radiation and enrich higher frequencies.
- We train a FNO model (Figure 2) where the target output is *Dynamic STF* and the input is the corresponding *best fitted Yoffe STF* (Figure 1 bottom right). Figure 5 show an example of estimations by the ML model.

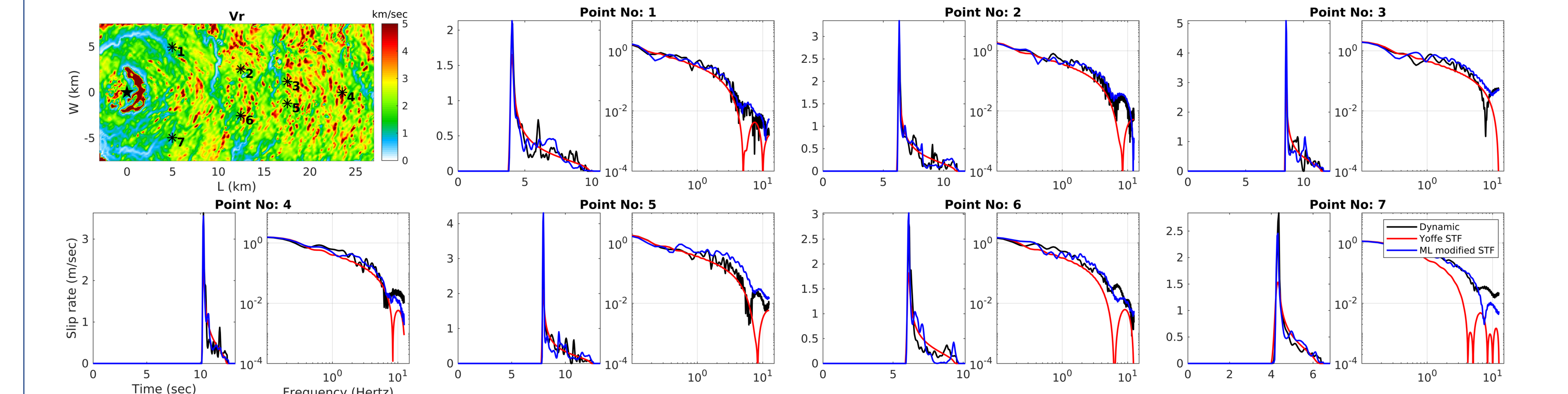


Figure 5. Modified version of Yoffe STF estimated using ML.

4 Scenario event

- To validate our rupture generator, we generate stochastic source model with steps outlined below.
- Random slip and hypocenter location for a hypothetical M_w 6.5 earthquake scenario following Mai and Beroza (2002) and Mai et al., (2005) respectively.
- Machine Learning models to compute V_r , PSV , Tr and STF modifications (Figures 6 and 7).

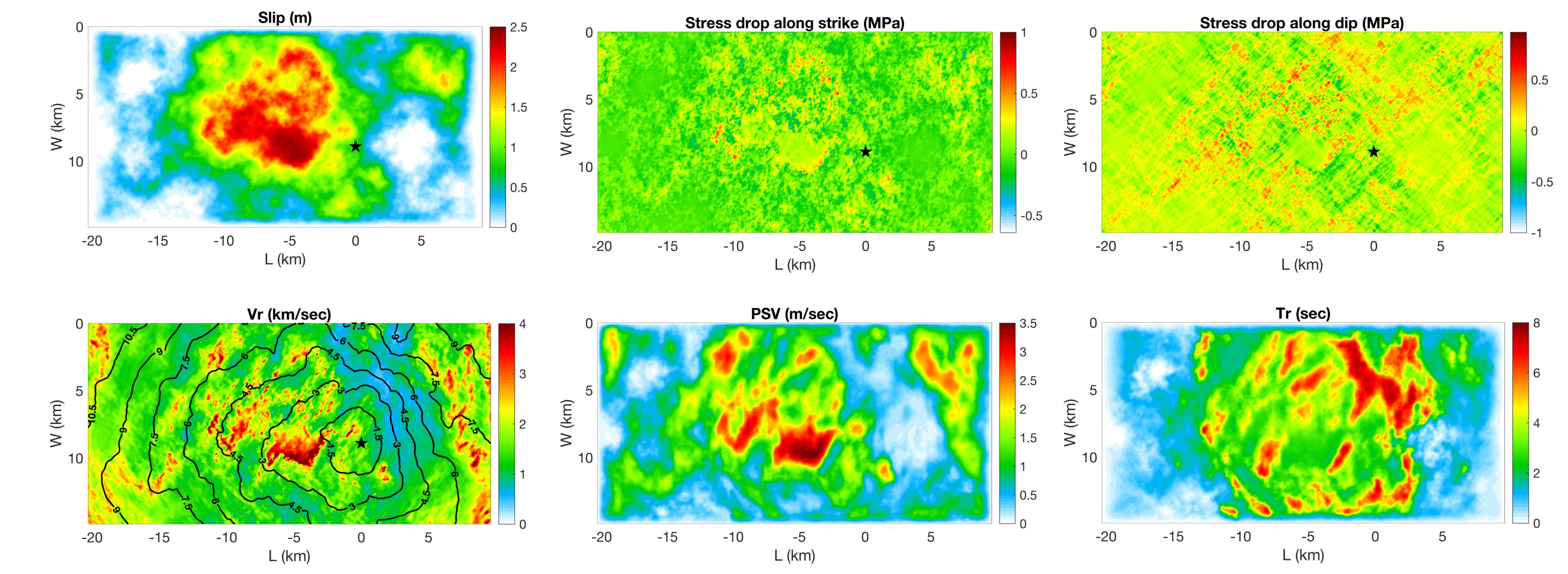


Figure 6. Kinematic source parameters for a hypothetical M_w 6.5 strike-slip earthquake. We begin with a random slip (Mai and Beroza (2002)) and a slip-conditioned hypocenter location (Mai et al., 2005). Thereafter, we compute the static on-fault stress drop. Parameters V_r , PSV and Tr are obtained using a ML approach.

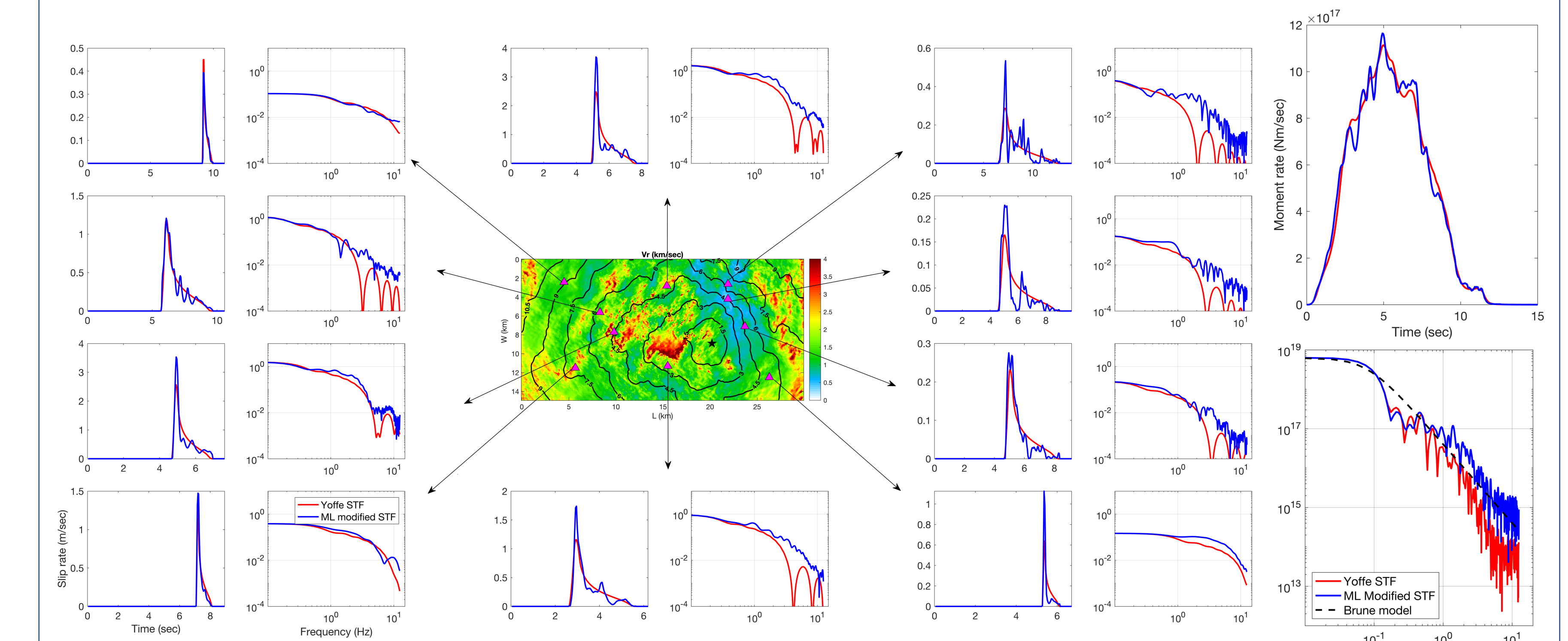


Figure 7. ML estimations of modified STFs. Blue curves are modifications to Yoffe STF shown in red. Total moment rate is shown in top right. Adding variations makes source spectrum more closely follow Brune's model (bottom right).

5 Ground motion simulations and validation

- We perform ground motion simulations in a 1D layered medium (Graves and Pitarka (2016)) with resolved max. frequency of 8 Hz (Figure 8).
- We account for anelastic attenuation using frequency dependent power law.
- PGV shakemap and velocity ground motions (Figure 8) highlight local and global directivity effects.
- We compare RotD50 spectral accelerations with 4 NGA West2 GMMs (Figure 8).

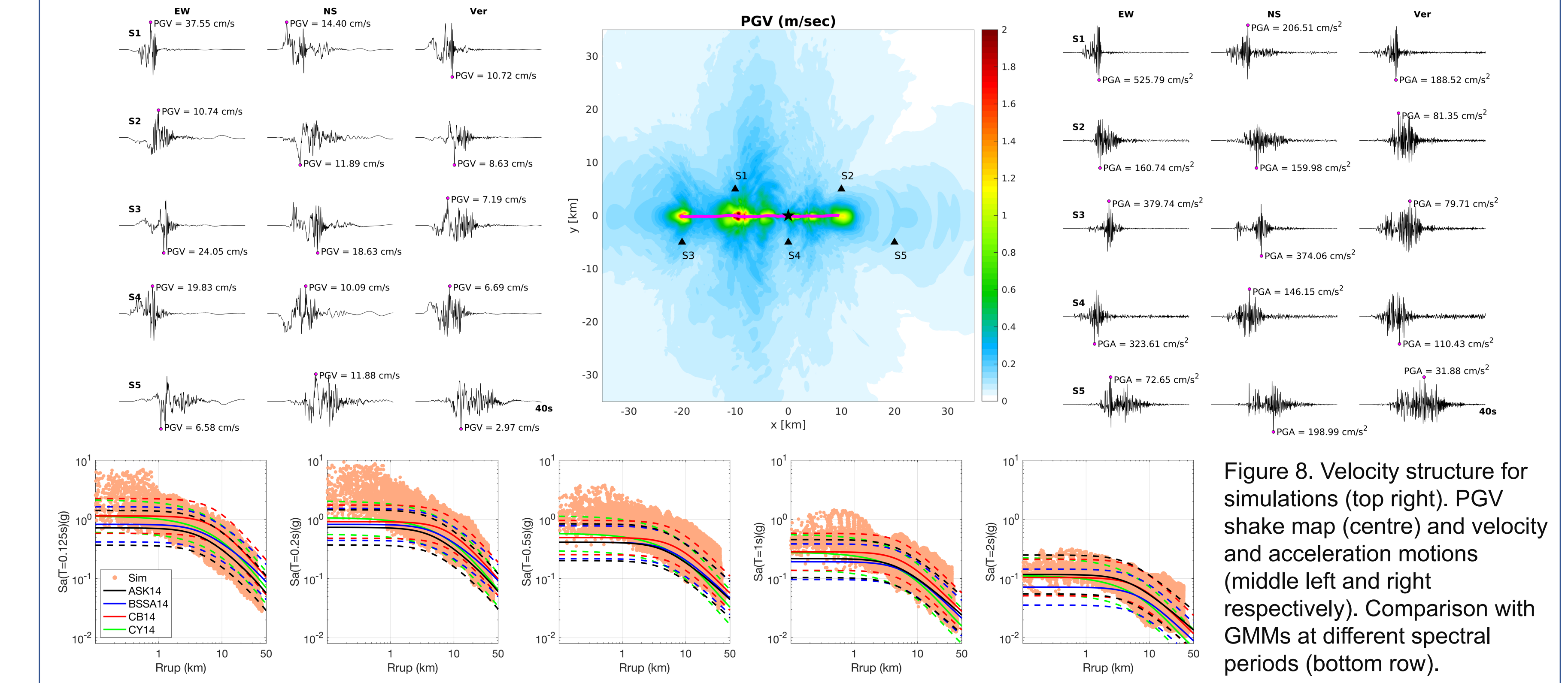


Figure 8. Velocity structure for simulations (top right), PGV shake map (centre) and velocity and acceleration motions (middle left and right respectively). Comparison with GMMs at different spectral periods (bottom row).

6 Conclusions

- Our Pseudo-dynamic rupture generator enables a full spatio-temporal characterization of earthquake source that accounts for dynamic rupture on rough faults and conditioned only on slip and hypocenter location .
- Simulations of M_w 6.5 strike slip scenario show global and local directivity effects.
- The simulations follow GMMs at distances larger than about $R \sim 3-5$ km. At short distances and high frequencies, our simulated motions are higher than GMM-estimates, which we attribute to two effects: (i) missing 3D effects, and seismic scattering in wave-propagation; (ii) incomplete datasets of near-field ground-motion recordings for GMM-development.

References

1. Guatteri, M., Mai, P. M., & Beroza, G. C. (2004). A pseudo-dynamic approximation to dynamic rupture models for strong ground motion prediction. *Bulletin of the Seismological Society of America*, 94(6), 2051–2063.
2. Graves, R. W., & Pitarka, A. (2010). Broadband ground-motion simulation using a hybrid approach. *Bulletin of the Seismological Society of America*, 100(5A), 2095–2123.
3. Graves, R. W., & Pitarka, A. (2015). Kinematic ground-motion simulations on rough faults including effects of 3D stochastic velocity perturbations. *Bulletin of the Seismological Society of America*.
4. Song, S.-G., Dalguer, L. A., & Mai, P. M. (2013). Pseudo-dynamic source modeling with 3-point and 2-point statistics of earthquake source parameters. *Geophysical Journal International*, 196(3), 1770–1786.
5. Mai, P. M., Gollis, M., Thirupajiam, K. K. S., Vyas, J. C., & Dunham, E. M. (2018). Accounting for fault roughness in pseudo-dynamic ground-motion simulations. *Pure and Applied Geophysics* (PAGEOPH), 174(9), 3419–3450.
6. Zongyi Li, Nikita Kovachik, Kamraj Azizadineheli, Burjude Liu, Kaushik Bhattacharya, Andrew Stuart, and Animes Anandkumar. Fourier neural operator for parametric partial differential equations, 2020.
7. Andrews, D. J. (2005). Rupture dynamics with energy loss outside the slip zone. *Journal of Geophysical Research*, 110, B03307.
8. Tinti, E., Fukuyama, E., Piatanesi, A., & Cocco, M. (2005). A kinematic source-time function compatible with earthquake dynamics. *Bulletin of the Seismological Society of America*, 95, 1211–1223.
9. Mai, P. M., & Beroza, G. C. (2002). A spatial random field model to characterize complexity in earthquake slip. *Journal of Geophysical Research*, 107(B11), 2308.
10. Mai, P. M., Spudich, P., Boatwright, J. L. Hypocenter Locations in Finite-Source Rupture Models. *Bulletin of the Seismological Society of America* 2001, 91(3): 965–980.